

Histopathological and Immunohistochemical Studies of Lesions Associated with Ebola Virus in a Naturally Infected Chimpanzee

M. Wyers, P. Formenty, Y. Cherel, L. Guigand,
B. Fernandez, C. Boesch, and B. Le Guenno

Laboratoire d'histopathologie animale, Ecole nationale vétérinaire, Nantes, and World Health Organization (WHO) Collaborating Center for Arboviruses and Haemorrhagic Fevers, Institut Pasteur, Paris, France; WHO, Tai Forest Project, and Centre Suisse de recherches scientifiques, Abidjan, Côte d'Ivoire

Lesions caused by the Côte d'Ivoire subtype of Ebola virus in a naturally infected young chimpanzee were characterized by histopathological and immunohistochemical methods. The predominant lesions consisted of multifocal necrosis in the liver and diffuse fibrinoid necrosis in the red pulp of the spleen. In these sites, macrophages contained large eosinophilic intracytoplasmic inclusion bodies. Immunohistochemical staining indicated that macrophages were a major site of viral replication. The absence of bronchiolar and pulmonary lesions and the paucity of antigen-containing macrophages in the lung suggested that aerosol transmission by this animal was unlikely. There were necrotic foci and antigen-containing macrophages in intestinal lymph nodes, in association with lesions caused by intestinal parasites, suggesting the possibility of virus entry through the digestive tract.

A new subtype of Ebola (EBO) filovirus designated EBO (subtype Côte d'Ivoire [EBO-CI]) was isolated from a researcher who was probably infected in late 1994 during the necropsy of a chimpanzee (*Pan troglodytes verus*) [1]. The animal was a member of a free-ranging community living in Taï National Park, Côte d'Ivoire, that has been studied since 1979. EBO-CI appears to be a new subtype of EBO filovirus, and it is antigenically different from the 3 subtypes that were isolated during previous hemorrhagic fever outbreaks in the Democratic Republic of the Congo, Sudan, and the United States [1]. The Zaire and Sudan subtypes (EBO-Z and EBO-S, respectively) were derived from human cases and appeared highly lethal for human [2–6] and nonhuman primates [7]. The Reston subtype (EBO-R), which was isolated from a cynomolgus monkey (*Macaca fascicularis*) colony, appeared to be lethal for nonhuman primates and nonpathogenic for humans [8, 9]. EBO-CI expresses a new pathogenic potential: It seems to be highly lethal for chimpanzees and clearly pathogenic but apparently nonlethal for humans. This fact suggests that neither nonhuman primates nor humans are natural hosts of EBO virus.

To help elucidate the pathogenesis of EBO infection in naturally infected chimpanzees, we now describe histological findings in lesions in selected tissues and immunohistochemical localizations of EBO-CI.

Materials and Methods

The chimpanzee that we studied was a 45-month-old female, who was necropsied after being found dead in November 1994.

Reprints or correspondence: Dr. M. Wyers, Laboratoire d'histopathologie animale, Ecole nationale vétérinaire, BP40706, 43307 Nantes Cedex 03, France (wyers@vet-nantes.fr).

The Journal of Infectious Diseases 1999;179(Suppl 1):S54–9
© 1999 by the Infectious Diseases Society of America. All rights reserved.
0022-1899/99/79S1-0011\$02.00

Lesions on the animal suggested hemorrhagic septicemia, so pertinent laboratory analyses were done, especially histological studies of different tissues. The nervous system, endocrine glands, skin, genitalia, and lymph nodes (except for a few small parietal nodes collected with the gut) were not examined histologically. Selected tissues were fixed in 10% buffered neutral formalin and embedded in paraffin according to routine procedures. All histological sections (4 μ m thick) were stained with hematoxylin-eosin-saffron. The Lendrum method of identifying red-stained polymerized fibrin deposits and Perl's method for using ferroprotein pigments were also used for selected slides.

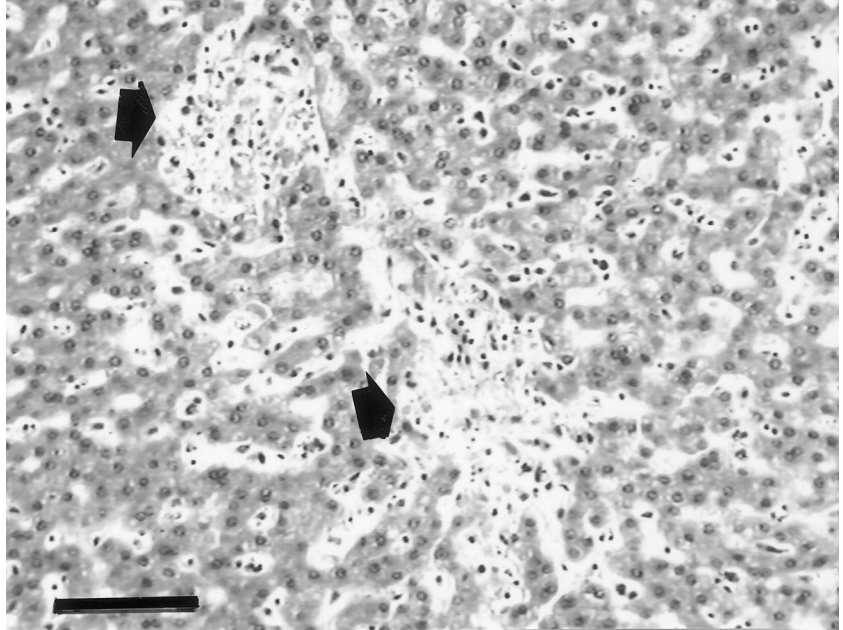
Immunohistochemical studies were done on paraffin-embedded slides for selected tissues, using two mouse polyclonal antibodies (Institut Pasteur), one of which was prepared with EBO-CI and the other with a recombinant N protein from the Gabon strain (an EBO-Z), which is known to cross-react with EBO-CI. Antibody dilutions of 1:140 and 1:200, respectively, were used.

An immunoperoxidase staining technique was performed using the streptavidin-biotin complex amplification system with 3',3'-diaminobenzidine as the chromogen. Sections were previously treated with 10% hydrogen peroxide for 3 min at 37°C to eliminate endogenous peroxidases. Primary antibodies were incubated for 90 min. Biotin-labeled secondary antibody was incubated for 1 h, after which streptavidin-peroxidase was added for another h; color in the sections was then detected using 3',3'-diaminobenzidine as the chromogen (kit K 391; Dako, Trappes, France). Negative control slides were made using the same method; however, they were not incubated with the primary antibody. To check for possible nonspecific reactions with polyclonal antibodies, we conducted a competition test using viral antigen. The inactivated viral antigen was a lysate of infected Anorat cells treated with 1% Triton. The viral preparation was diluted 1:1000 and mixed in equal parts with diluted antibody in PBS (pH 7.6), and 2% bovine serum albumin was added.

Results

Although fixation of tissue for histological examination was done a short time after the death of the chimpanzee, tissues had

Figure 1. Hematoxylin-eosin-saffron staining of liver of Ebola-infected chimpanzee (scale: 100 μm). Arrows indicate necrotic foci of hepatic parenchyma. Necrotic hepatic cells have disappeared; inflammatory cell infiltration is moderate. Dark nuclei of Kupffer's cells are apparent in sinusoid spaces. Original magnification $\times 189$.

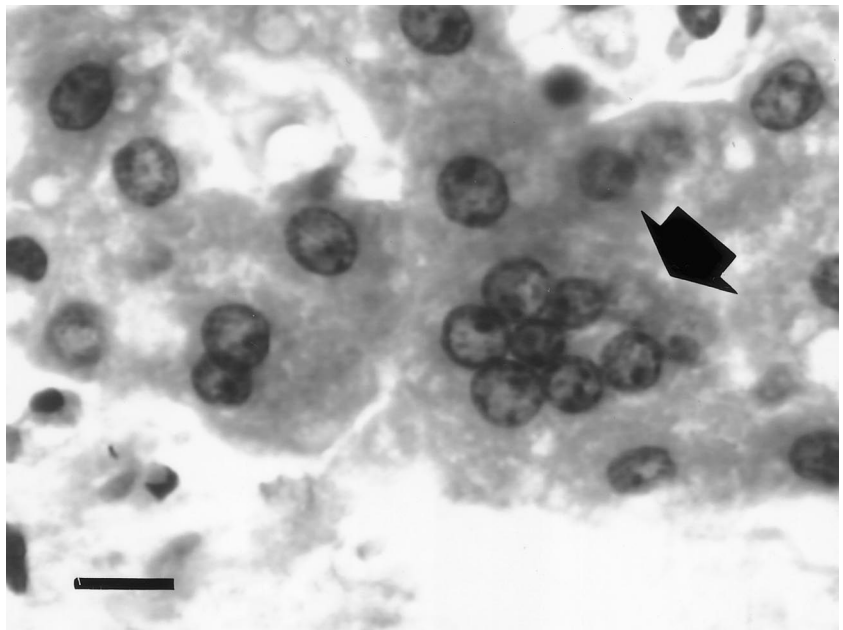


undergone autolytic changes because of the hot local climate. Autolysis was especially evident in renal parenchyma, digestive mucosa, and myocardial cells and interfered with the analyses of possible degenerative lesions in these tissues. However, the relevant analysis of lesions was possible for all other tissues.

Liver lesions consisted of numerous small necrotic foci moderately infiltrated with inflammatory cells and randomly distributed in the hepatic lobules (figure 1). One of the most obvious changes in hepatocytes was the formation of numerous multinucleated syncytia of hepatic cells (figure 2). Multinucleated

cells were disseminated randomly throughout the normal parenchyma. Concurrently, the hepatic parenchyma exhibited obvious diffuse hyperplasia of Kupffer's cells (figure 1). Single, large, and poorly defined highly acidophilic hyalin inclusion bodies were identified in the cytoplasm of circulating and vascular macrophages disseminated throughout the hepatic parenchyma (figure 3). Despite their poorly defined features, these macrophagic intracytoplasmic inclusion bodies can probably be considered viral inclusions. The cytoplasm of many hepatic macrophages contained granular deposits of brown pigment,

Figure 2. Hematoxylin-eosin-saffron staining of liver of Ebola-infected chimpanzee (scale: 10 μm). Arrow indicates syncytial, multinucleated cell containing 8 nuclei; binucleated hepatic cell is to its left. Original magnification $\times 1190$.



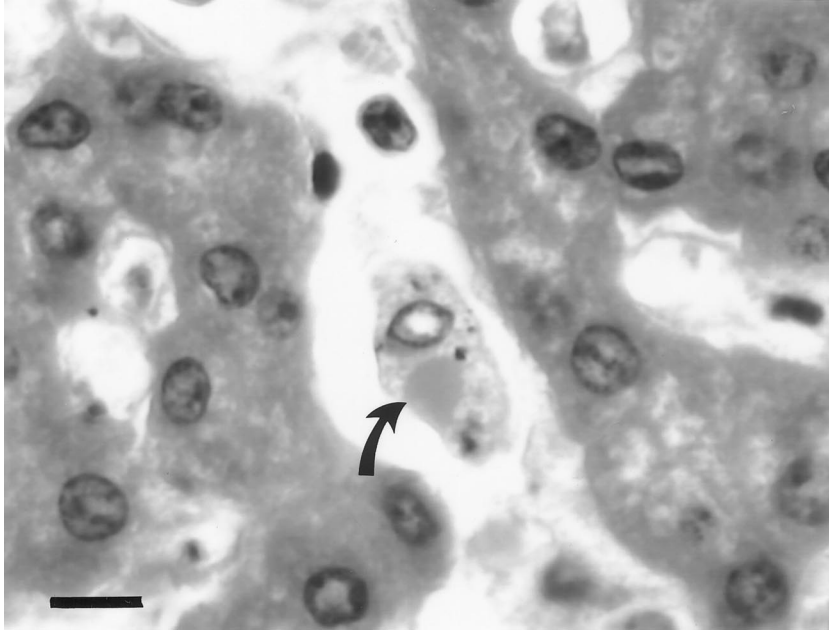


Figure 3. Hematoxylin-eosin-saffron staining of liver of Ebola-infected chimpanzee (scale: 10 μm). Arrow indicates large, eosinophilic hyalin inclusion body in cytoplasm of circulating macrophage in sinusoid capillary. Original magnification $\times 1190$.

which appeared to be hemosiderin and which stained blue by Perl's method. No vascular lesions (e.g., interstitial and capsular hemorrhages or capillary and venous thromboses) were observed in the hepatic parenchyma, even when a fibrin-specific staining method was used.

Incubation of hepatic parenchyma with the two antibodies revealed a moderate number of positive cells with diffusely brown cytoplasm, all of which were free or vascular macrophages. Immunoperoxidase staining disappeared in macrophages when antigenic competition was performed. Immunocytochemical methods failed to reveal any obvious specific deposits in hepatic cell cytoplasm. Cytoplasmic inclusion bodies, observed in hepatic macrophage cytoplasm, were stained slightly with EBO-CI mouse antibody but intensely with the other mouse serum. The inclusion bodies were not stained after the viral antigenic competitive method. The largest inclusion bodies generally displayed an amorphous, pale, unstained center, with antigen deposits concentrated exclusively at the periphery; a few inclusion bodies were totally negative for viral antigen. Extracellular, diffuse brown-stained deposits that were specific for EBO antigens after antigenic competition were seen in necrotic foci in conjunction with necrotic changes.

The spleen exhibited marked congestion and extensive areas of fibrinoid and hemorrhagic necrosis of the red pulp. Fibrinoid necrotic areas mixed with numerous red blood cells were more apparent in the marginal zones surrounding lymphoid follicles. Depletion of lymphoid cells was obvious in almost all lymphoid follicles, sometimes concurrently with pyknosis or karyorrhexis of lymphoid cell nuclei (figure 4). The cytoplasm of numerous splenic macrophages contained large, amorphous, acidophilic material that was similar to the inclusion bodies observed in macrophages of hepatic parenchyma; most of this material ap-

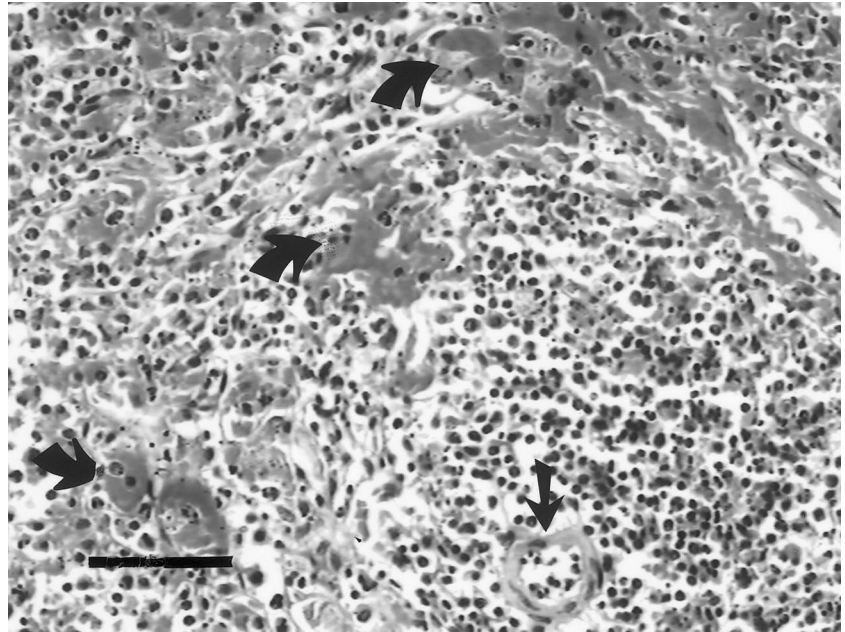
peared sufficiently characteristic to be regarded as intracytoplasmic viral inclusions.

Immunocytochemical staining gave the same results as those for hepatic parenchyma: The cytoplasm of numerous macrophages was specifically immunopositive with the two antibodies used. Specific staining could not be conclusively detected in characteristic lymphocyte cells. The necrotic areas, especially around lymphoid follicles, displayed specific, highly brown-stained extracellular deposits. Immunocytochemical staining of splenic intracytoplasmic inclusion bodies revealed the same features as found in hepatic viral inclusions (figure 5).

Strongly positive granular deposits, observed with both mouse polyclonal antibodies in the perinuclear area of biliary epithelial cells and in the cytoplasm of endothelial cells of spleen sinusoids, were nonspecific and still brown-stained after the antigenic competition test. Some macrophage nuclei also showed nonspecific staining.

The gastric and intestinal mucosae exhibited extensive autolytic changes. Numerous sections of nematode parasites were seen free within the intestinal lumen. A mild diffuse infiltration of the lamina propria and the submucosa by mononuclear inflammatory cells was observed in all examined sections of the gut. Diffuse inflammation was associated with several delimited pyogranulomatous lesions of the intestinal wall, with a large infiltration of activated macrophages mixed with neutrophilic and many eosinophilic granulocytes. Sections of more or less disintegrated nematode parasites, surrounded by suppurative infiltration, were also observed in the center of one of the intestinal granulomatous lesions. An obvious hyperplasia of the lymphoid follicles of Peyer's patches, associated with moderate pyknosis of the centrofollicular lymphoid cells, was seen. We could not detect any convincing evidence of inclusion

Figure 4. Hematoxylin-eosin-saffron staining of spleen of Ebola-infected chimpanzee (scale: 50 μ m). Arrow at bottom right indicates transverse section of follicular artery in lymphoid follicle. Curved arrows indicate several foci of fibrinoid necrosis of red pulp surrounding lymphoid follicle. Lymphoid follicle displays lymphoid cell depletion, with several pyknotic lymphocytic nuclei. Original magnification $\times 315$.



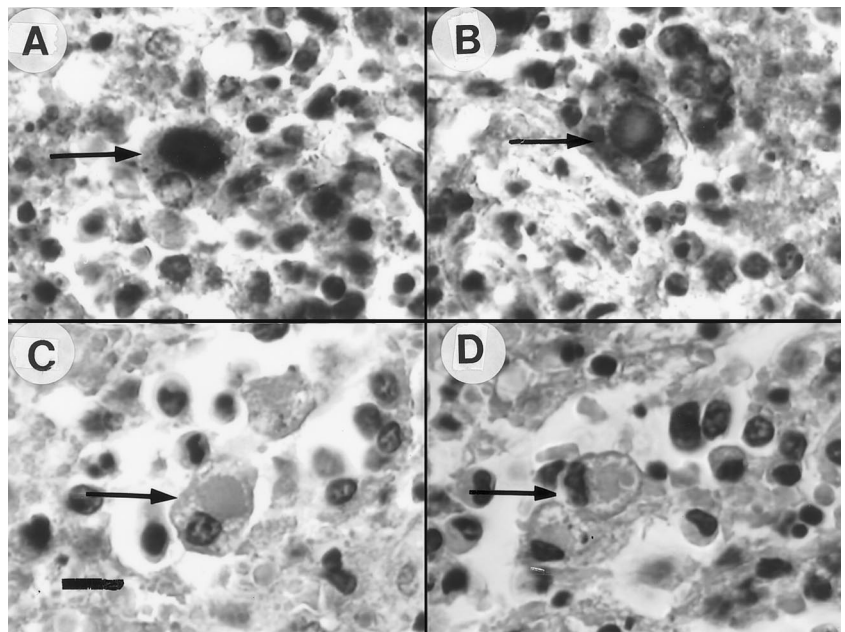
bodies in the macrophage population of Peyer’s patches in routinely stained slides. No specific positive macrophages were identified in the walls or in Peyer’s patches of the digestive tract after immunochemical labeling. Numerous granular deposits were revealed (by nonspecific staining after the antigenic competition test) in the perinuclear cytoplasm of the glandular part of the gastric and intestinal epithelium.

Small parietal lymph nodes were removed with the gut. The centrofollicular areas of the lymphoid follicles exhibited focal

pyknotic and necrotic changes. Immunohistological methods revealed few macrophages with positively stained (brown) cytoplasm in the cortical and medullar sinuses of lymph node pulp.

Blood stasis and intraalveolar terminal edema were seen in lung parenchyma. Mild chronic emphysema with small foci of subpleural atelectasis was also observed, but no thrombotic, vascular, or hemorrhagic lesions were found. Bronchial and bronchiolar mucosae were normal. No inclu-

Figure 5. Immunoperoxidase staining, using antibody of Gabon strain (an EBO-Z), of spleen from Ebola-infected chimpanzee (scale: 20 μ m). **A**, Staining (antibody dilution of 1/200) revealed (see arrow) voluminous viral inclusion, which was totally stained bright brown by antibody, in cytoplasm of macrophage of red pulp. **B**, Staining (antibody dilution of 1/200) revealed (see arrow) viral inclusion with peripheral deposit of viral antigen and which was slightly more stained by antibody than was viral inclusion in **A**. **C**, Staining with viral antigen. Viral inclusion in macrophage appears unstained (arrow) after competition test. Result indicates specificity of polyclonal antibody used. **D**, Negative control that was not incubated with primary antibody. Intracytoplasmic viral inclusion appears unstained (arrow; compare with **C**). Original magnification $\times 402$.



sion bodies could be definitely identified in any pulmonary cell populations. The cytoplasm of only a few free alveolar macrophages was specifically labeled by immunochemical staining methods.

Cardiomyocytes displayed obvious anisokaryosis, with some well-defined nucleolated nuclei twice the normal size. Immunopositive macrophages were not detected in the myocardial parenchyma.

Extensive, diffuse autolytic changes prevented the identification of epithelial tubular alterations in the kidney; however, no inflammatory or vascular lesions were observed in the renal parenchyma. Fibrin-specific staining failed to reveal fibrin thrombi in glomerular capillaries, even in blood vessels of the cortex and outer medulla. Immunopositive macrophages were not identified in the interstitium of renal parenchyma.

Discussion

A limited number of tissue specimens that were selected routinely during the animal necropsy were available for this study; thus considerations about the route of viral infection were limited. Moreover, all tissue samples were fixed in formalin and embedded in paraffin, which reduced the possibility of other types of examinations. Finally, despite the relatively short period between death and necropsy, obvious autolytic changes occurred, which could have led to misinterpretation in tissues such as kidney or digestive tract, known to be susceptible to early autolysis.

Two different mouse polyclonal antibodies were used for immunochemical detection of viral antigens. Both reacted similarly, indicating the presence of viral antigen in the cytoplasm of macrophages. Only macrophages were immunopositive in the present study, especially resident macrophages of spleen, liver, and circulating cells. As described previously in experimental cases, lymphocytes and epithelial cells were apparently unaffected; the present case provides significant additional information confirming that the main target of viral infection is the macrophage system, which appears to be the most important site of viral replication [10, 11].

There were numerous inclusion bodies in splenic and hepatic macrophages. They were single, large, amorphous, and acidophilic and were very similar to the viral inclusions observed in natural or experimental diseases [7, 9, 11, 12]. However, because of their morphology, intracytoplasmic eosinophil material could be easily confused in routinely stained slides with phagocytic bodies within the cytoplasm of macrophages, especially those near the foci of fibrinoid necrosis. Thus, complementary immunohistochemical techniques were very useful for establishing the diagnosis of their viral origin.

All inclusion bodies did not react equally to immunochemical staining. The smallest were consistently stained completely brown, whereas the larger inclusions, as previously described by Le Guenno et al. [1], displayed strongly immu-

nopositive staining only on the periphery, with an unstained central area apparently free of viral antigen. Moreover, a few inclusion bodies were totally negative for viral antigen. The few free viral intracytoplasmic inclusions observed may be considered to be cellular structures that are different from specific viral inclusion bodies and possibly identical to the intracytoplasmic nonviral tubuloreticular inclusions described by Geisbert et al. [10] in electron microscopy studies. Nevertheless, our observation of intermediate stages between immunopositive and immunonegative inclusions suggests a progressive elimination of virus particles, leading to immunonegative inclusion bodies.

Aerosol transmission of filovirus in monkeys has been demonstrated in spontaneous [13] and experimental cases [14]; however, the prominent pneumonic component of the disease in lung-infected monkeys was lacking in our case, and only a few immunoreactive macrophages were seen in the pulmonary parenchyma, suggesting that aerosol transmission was not the main route of infection. The severity of the digestive pyogranulomatous parasitic lesions associated with multifocal acute necrotic changes in parietal lymph nodes suggested the possibility of viral entry through the digestive tract. The occurrence of a lethal experimental infection in rhesus monkeys by the oral and conjunctival routes after exposure to EBO-Z lends support to this hypothesis [11]. Moreover, the diet of the chimpanzee supported the hypothesis that infection might have been introduced via the digestive tract: The young female had been nursed by her mother, who disappeared a week before, probably as the result of an EBO virus infection.

As previously reported by Fischer-Hoch et al. [15], the course of the disease and the intensity of clinical symptoms and pathological lesions in experimental conditions depend on the virus strain. The course of infection with EBO-Z and EBO-S (African filoviruses) is accelerated and often more severe than with EBO-R or the Pennsylvania strain (Asian filoviruses). On the other hand, host response also contributes to the severity of infection: African green monkeys appear less susceptible to severe or fatal disease than do cynomolgus monkeys. The lesions described in the present report are similar to those observed in spontaneous viral hemorrhagic fever in humans [16] and in monkeys naturally and experimentally infected with EBO viruses [7–12, 14]. Nevertheless, necrotic lesions and viral antigen tissue distribution appeared to be less extensive and severe, and hemorrhagic, thrombotic, or vascular lesions suggestive of disseminated intravascular coagulation were never noted. This observation raises certain questions about the pathophysiology of the new subtype of EBO virus (i.e., EBO-CI) in humans and apes.

References

1. Le Guenno B, Formenty P, Wyers M, Gounon P, Walker F, Boesch C. Isolation and partial characterization of a new strain of Ebola virus. *Lancet* 1995;345:1271–3.

2. Johnson K, Lange L, Murphy F. Isolation and partial characterization of a new virus causing acute haemorrhagic fever in Zaire. *Lancet* **1977**;1: 569–71.
3. Report of WHO International Study Team. Ebola hemorrhagic fever in Zaire, 1976. *Bull World Health Organ* **1978**;56:247–70.
4. Report of WHO International Study Team. Ebola hemorrhagic fever in Sudan, 1976. *Bull World Health Organ* **1978**;56:271–93.
5. Heymann D, Weisfeld J, Webb P, Johnson K, Cairns T, Berquist H. Ebola hemorrhagic fever, Tandala, Zaire, 1977–78. *J Infect Dis* **1980**;142: 372–6.
6. Baron R, McCormick J, Zubeir O. Ebola virus disease in southern Sudan: hospital dissemination in intrafamilial spread. *Bull World Health Organ* **1983**;61:997–1003.
7. Baskerville A, Bowen ETW, Platt GS, McArdeLL LB, Simpson DIH. The pathology of experimental Ebola virus infection in monkeys. *J Pathol* **1978**;125:131–8.
8. Jahrling PB, Geisbert TW, Dalgard DW, et al. Preliminary report: isolation of Ebola virus from monkeys imported in USA. *Lancet* **1990**;335: 502–5.
9. Jahrling PB, Geisbert TW, Jaax NK, Hanes MA, Ksiazek TG, Peters CJ. Experimental infection of cynomolgus macaques with Ebola-Reston filovirus from 1989–1990 US epizootic. *Arch Virol* **1996**; (suppl)11: 115–34.
10. Geisbert TW, Jarhling PB, Hanes MA, Zack PM. Association of Ebola-related Reston virus particles and antigen with tissue lesions of monkeys imported to the United States. *J Comp Pathol* **1992**;106: 137–52.
11. Jaax NK, Davis KJ, Geisbert T, et al. Lethal experimental infection of rhesus monkeys with Ebola-Zaire (Mayinga) virus by the oral and conjunctival route of exposure. *Arch Pathol Lab Med* **1996**;120: 140–55.
12. Murphy FA. Pathology of Ebola virus infection. In: SR Pattyn, ed. Ebola virus haemorrhagic fever. Amsterdam: Elsevier/North-Holland, **1978**: 37–42.
13. Dalgard DW, Hardy RJ, Pearson SL, et al. Combined simian hemorrhagic fever and Ebola virus infection in cynomolgus monkeys. *Lab Anim Sci* **1992**;42:152–7.
14. Johnson E, Jaax N, White J, Jarhling P. Lethal experimental infection of rhesus monkeys by aerosolized Ebola virus. *Int J Exp Pathol* **1995**;76: 227–36.
15. Fischer-Hoch SP, Brammer TL, Trappier SG, et al. Pathogenic potential of filoviruses: role of geographic origin of primate host and virus strain. *J Infect Dis* **1992**;166:753–63.
16. Fischer-Hoch SP, Platt GS, Neild GH, et al. Pathophysiology of shock and hemorrhage in a fulminating viral infection (Ebola). *J Infect Dis* **1985**;152:887–94.